JVI Journals.ASM.org

Prion Infectivity Plateaus and Conversion to Symptomatic Disease Originate from Falling Precursor Levels and Increased Levels of Oligomeric PrP^{Sc} Species

Charles E. Mays,[a] Jacques van der Merwe,[a] Chae Kim,[b] Tracy Haldiman,[b,c] Debbie McKenzie,[a,e] Jiri G. Safar,[b,c,d] David Westaway[a,e,f]

Centre for Prions and Protein Folding Diseases, University of Alberta, Edmonton, Alberta, Canada[a]; National Prion Disease Pathology Surveillance Center,[b] Department of Pathology,[c] and Department of Neurology, School of Medicine, Case Western Reserve University, Cleveland, Ohio, USA[d]; Department of Biological Sciences, Division of Neurology,[e] and Department of Biochemistry,[f] University of Alberta, Edmonton, Alberta, Canada

ABSTRACT

In lethal prion neurodegenerative diseases, misfolded prion proteins (PrP^{Sc}) replicate by redirecting the folding of the cellular prion glycoprotein (PrP^{C}). Infections of different durations can have a subclinical phase with constant levels of infectious particles, but the mechanisms underlying this plateau and a subsequent exit to overt clinical disease are unknown. Using tandem biophysical techniques, we show that attenuated accumulation of infectious particles in presymptomatic disease is preceded by a progressive fall in PrP^{C} level, which constricts replication rate and thereby causes the plateau effect. Furthermore, disease symptoms occurred at the threshold associated with increasing levels of small, relatively less protease-resistant oligomeric prion particles ($oPrP^{Sc}$). Although a hypothetical lethal isoform of PrP cannot be excluded, our data argue that diminishing residual PrP^{C} levels and continuously increasing levels of $oPrP^{Sc}$ are crucial determinants in the transition from presymptomatic to symptomatic prion disease.

IMPORTANCE

Prions are infectious agents that cause lethal brain diseases; they arise from misfolding of a cell surface protein, PrP^{C} to a form called PrP^{Sc}. Prion infections can have long latencies even though there is no protective immune response. Accumulation of infectious prion particles has been suggested to always reach the same plateau in the brain during latent periods, with clinical disease only occurring when hypothetical toxic forms (called PrP^{L} or TPrP) begin to accumulate. We show here that infectivity plateaus arise because PrP^{C} precursor levels become downregulated and that the duration of latent periods can be accounted for by the level of residual PrP^{C}, which transduces a toxic effect, along with the amount of oligomeric forms of PrP^{Sc}.

Prions are proteinaceous, infectious particles responsible for a group of incurable neurodegenerative diseases in humans and animals. A posttranslationally misfolded version of the cellular prion protein (PrP^{C}), known as PrP^{Sc}, is the primary component of a prion and propagates by acting as a template for the conformational conversion of PrP^{C} substrate (1). Analysis of brain material by prion bioassays has shown that infectivity plateaus can exist early during disease, suggesting that infections can be divided into an infectivity phase and a toxicity phase (2–4). The accumulation of a hypothetical toxic PrP form (PrP^{L}, "L" for lethal), distinct from PrP^{Sc}, has been proposed to explain the transition from a subclinical phase to the appearance of clinical signs and progression to end-stage disease at the time when the prion levels plateau. It has been further suggested that prions are infectious, but nontoxic, entities that act as a catalyst for the generation of toxic PrP^{L} at a rate with direct proportionality to PrP^{C} expression levels in the animal models used for these experiments (2). However, this hypothetical protein has yet to be isolated.

In other studies, based on falling levels of the PrP-like Shadoo (Sho) protein, we recently demonstrated that the extended asymptomatic stage encompasses a different chemical parameter, namely, the posttranslational downregulation of PrP^{C} levels (5). We surmised that a functional relationship might exist between the PrP^{C} downregulation seen at disease endpoint ("ΔPrP^{C}," as measured against mock-infected control mice) in different prion diseases and the formation of PrP^{Sc} measured by conformation-dependent immunoassay (CDI) (5). We explored this relationship for RML, 139A, Sc237, and CJD prion isolates using an *in vitro* protein misfolding cyclic amplification system (6, 7). In titrated amplification reactions using low $rPrP^{Sc}$ concentrations (to model an early stage in disease), a 30% decrease in PrP^{C} substrate produced a 54% drop in replication rate (from 118- to 54-fold) of protease-resistant PrP^{Sc} (5). However, these earlier studies neither addressed the full time course of disease nor the formation of infectious prion particles. Here, we used standard scrapie cell assay (SSCA) data to better understand the relationship between the infectivity plateau and substrate reduction in mice of three genotypes.

MATERIALS AND METHODS

Mouse lines, prion bioassays, and brain homogenates. Tg*Prnp* mice (abbreviated to *Tg20* [8]), a low-expresser Tg line (Tg.*Prnp*-AL), wild-type (wt) mice ($Prnp^{+/+}$), and hemizygous *Prnp*-null mice ($Prnp^{0/+}$) were

Received 24 August 2015 Accepted 25 September 2015

Accepted manuscript posted online 30 September 2015

Citation Mays CE, van der Merwe J, Kim C, Haldiman T, McKenzie D, Safar JG, Westaway D. 2015. Prion infectivity plateaus and conversion to symptomatic disease originate from falling precursor levels and increased levels of oligomeric PrP^{Sc} species. J Virol 89:12418–12426. doi:10.1128/JVI.02142-15.

Editor: B. W. Caughey

Address correspondence to David Westaway, david.westaway@ualberta.ca.

used as described previously (5) in accordance with the Canadian Council on Animal Care and were approved by the Institutional Animal Care and Use Committees at the University of Alberta. Mice were inoculated at ~6 weeks of age with 30 to 50 μl of 1% (wt/vol) brain homogenate containing RML mouse-adapted scrapie prions. The mice were sacrificed in a time course regimen designed to monitor changes in PrP and infectivity over the complete duration of the disease. These animals were monitored over this period for neurological signs associated with RML prion disease, including ataxia, a rigid tail, kyphosis, a bobbing head, and a rough coat. *Prnp*$^{0/+}$ mice were sacrificed on days 1 ($n = 4$), 60 ($n = 4$), 100 ($n = 4$), 140 ($n = 4$), 180 ($n = 4$; 0/4 were exhibiting prion disease symptoms), and 363 ($n = 2$) postinoculation when all animals reached terminal end-stage disease, as judged by symptomatic progression. *Prnp*$^{+/+}$ mice were sacrificed on days 1 ($n = 3$), 30 ($n = 3$), 60 ($n = 3$), 100 ($n = 3$), 140 ($n = 3$; first symptomatic time point for 2/3), and 162.67 ± 7.84 ($n = 3$) postinoculation when all animals reached terminal end-stage disease, as judged by symptomatic progression. *Tg20* mice were sacrificed on days 1 ($n = 3$), 15 ($n = 3$), 30 ($n = 3$), 45 ($n = 3$), 60 ($n = 3$; first symptomatic time point for 2/3), and 65 ($n = 3$) postinoculation when all animals reached terminal end-stage disease, as judged by symptomatic progression. Brain homogenate was made by serial passage through needles at 10% (wt/vol) in phosphate-buffered saline (PBS; pH 7.4).

Sucrose gradient evaluation. Velocity gradient centrifugation was used to separate monomeric, oligomeric, and high molecular assemblies of PrP as previously described (5). Briefly, the 400-μl aliquots of 10% brain homogenate containing 2% Sarkosyl were clarified and applied to a 10 to 45% sucrose gradient prepared in PBS (pH 7.4) containing 1% Sarkosyl. Ultracentrifugation was performed at 237,000 × *g* for 73 min at 5°C. Gradient fractions were bottom harvested.

CDI evaluation of PrP^C and PrP^{Sc} levels, replication rate, and specific infectivity. The validation of CDI has been reported by the authors and other laboratories (9–18). Here, we utilized the recently modified protocol that adapts CDI to murine samples (5). First, Lumitrac 600 High-Binding 96-well plates (E&K Scientific) were coated with monoclonal antibody (MAb) 8H4 (epitope 175-185) in 200 mM NaH_2PO_4 containing 0.03% (wt/vol) NaN_3 (pH 7.5) (19). Next, 20-μl aliquots from each fraction containing 0.007% (vol/vol) of Patent Blue V (Sigma-Aldrich) were directly loaded into wells prefilled with 200 μl of assay buffer (Perkin-Elmer). Then, the captured PrP was detected by europium-conjugated MAb 12B2 (epitope 88-92) (20). The time-resolved fluorescence (TRF) signals were measured by the multimode microplate reader PHERAstar Plus (BMG LabTech).

A calibration curve was prepared with either recombinant PrP(23-231, 129M) for samples containing full-length PrP^{Sc} or recombinant PrP(90-231, 129M) for samples containing truncated rPrP^{Sc} [PrP(27-30)] after proteinase K (PK) treatment. The PK-untreated sample containing PrP was divided into a native and a denatured aliquot, where the latter was denatured with 4 M guanidinium HCl for 5 min at 80°C. Using europium-labeled 12B2 for detection, the TRF signal of native samples corresponds to the epitope 88-92 that is exposed in α-helical PrP^C and hidden in PrP^{Sc}, thus allowing a direct measurement of the PrP^C concentration. The signal of the denatured aliquot corresponds to the total PrP in a sample. The concentration of PrP^{Sc} was calculated according to the following formula: $[PrP^{Sc}] = [PrP_D] - [PrP_N]$, where *D* stands for the denatured aliquot, and *N* stands for the native aliquot. Next, the concentration of rPrP^{Sc} was calculated in samples subjected to PK treatment, followed by complete denaturation using the PrP(90-231, 129M) calibration curve. The separate calibration for the PK-treated and untreated sample is critical for correct results due to the lower affinity of MAb 12B2 to denatured full-length human PrP(23-231, 129M) compared to PrP(90-231, 129M). Furthermore, the concentration of sPrP^{Sc} was calculated according the following formula: $[sPrP^{Sc}] = [PrP^{Sc}] - [rPrP^{Sc}]$. Replication was defined as the increase in the value of rPrP^{Sc} between two time points, thus allowing the replication rate to be deduced by determining the rate of change in the slope of the rPrP^{Sc} values as a dy/dx function. Lastly, specific infectivity was defined as the amount of infectious PrP^{Sc}, and determined by measuring the units of (SSCA-estimated) infectivity per mass of (CDI-estimated) PrP^{Sc} in the sample.

SSCA. SSCA was performed by exposing L929 cells to various concentrations of brain homogenates (0.1 to 0.0001% [wt/vol]) for 5 days in 96-well culture plates (5, 21). The cells were passaged three times (1:4 and 1:7), with 20,000 cells collected at the third passage and loaded on to MultiscreenHTS IP 96-well, 0.45-μm-pore-size filter plates (Millipore). Cells were subjected to PK digestion (5 μg/ml) and subsequent denaturation with 3 M guanidine thiocyanate. The enzyme-linked immunospot (ELISpot) reaction was performed using a mouse anti-PrP antibody (SAF83; 1:1,000) and a goat anti-mouse alkaline phosphatase-conjugated secondary antibody (1:5,000). The plates were developed using BCIP/NBT and analyzed using an Autoimmun Diagnostika GmbH ELISpot plate reader (ELR07). The plate reader was set at intensity 4, size 1, and gradient 0, using algorithm B; these settings produced a background noise level in control samples of fewer than 30 spots. Time course infectivity data are presented with a best-line fit by nonlinear regression plotted with GraphPad Prism software (sigmoidal function). Low-power views of ELISpot data from the three mouse genotypes were adjusted with the same parameters (−20% brightness, +40% contrast, and +50% sharpen).

RESULTS

Effect of PrP^C expression levels on the prion infectivity plateaus. Using brain homogenates derived from mice at end-stage with the Rocky Mountain Laboratory (RML) isolate of scrapie prions, we performed intracerebral inoculations on groups of mice expressing different levels of PrP^C: *Tg20* mice (also known as *tga*20) overexpressing PrP^C by ~6-fold (8), wild-type mice (wt; *Prnp*$^{+/+}$), and hemizygous *Prnp*-null mice (*Prnp*$^{+/0}$). Animals were sacrificed at designated time points throughout infection, including the terminal stage of disease. PrP^C levels from these time point studies (Fig. 1A) were determined as described previously (5), with the SSCA with L929 cells also being used to determine the prion infectivity of unfractionated brain homogenate (0.1% [wt/vol]) from animals at each time point (Fig. 1B). As expected, all three groups of animals exhibited a rapid exponential increase in infectivity early in the incubation period. However, while wt animals tended to plateau and a plateau could be clearly discerned in hemizygous mice, infectivity continued to rise until the *Tg20* overexpresser mice were scored as being in the terminal phase of disease. To assess whether the perceived decrease in replication rate for infectious titers in wt and hemizygous mice was merely derived from a "ceiling effect" of the assays performed in L929 cells, SSCA was repeated using a further 10-fold dilution of the brain homogenate samples (0.01% [wt/vol]). Here, the profiles of infectivity from the diluted samples resembled their more concentrated counterparts, arguing against such a ceiling effect (gray traces, Fig. 1B). In contrast to the concept of a single unifying plateau value for a given prion isolate measured in PK1 N2a cells (2, 3), the maximum values for titers measured in L929 cells differed significantly between wt and hemizygous mice with the same PrP allelic type (*Prnp*^{a}), where infectivity in wt mice was 1 log greater than hemizygous mice and 2 logs greater than *Tg20* mice ($P < 0.0001$ for both 0.1 and 0.01% homogenates; Table 1). Low-power views of representative ELISpot filters used for the time course analyses are presented in Fig. 1C to complement the numerical data of Fig. 1B and illustrate the plateau effect especially apparent in infected hemizygous mice.

Relationship between PrP^C downregulation and the prion infectivity plateau. Infectivity continued to rise to disease endpoint in time course studies of inoculated *Tg20* mice (Fig. 1B),

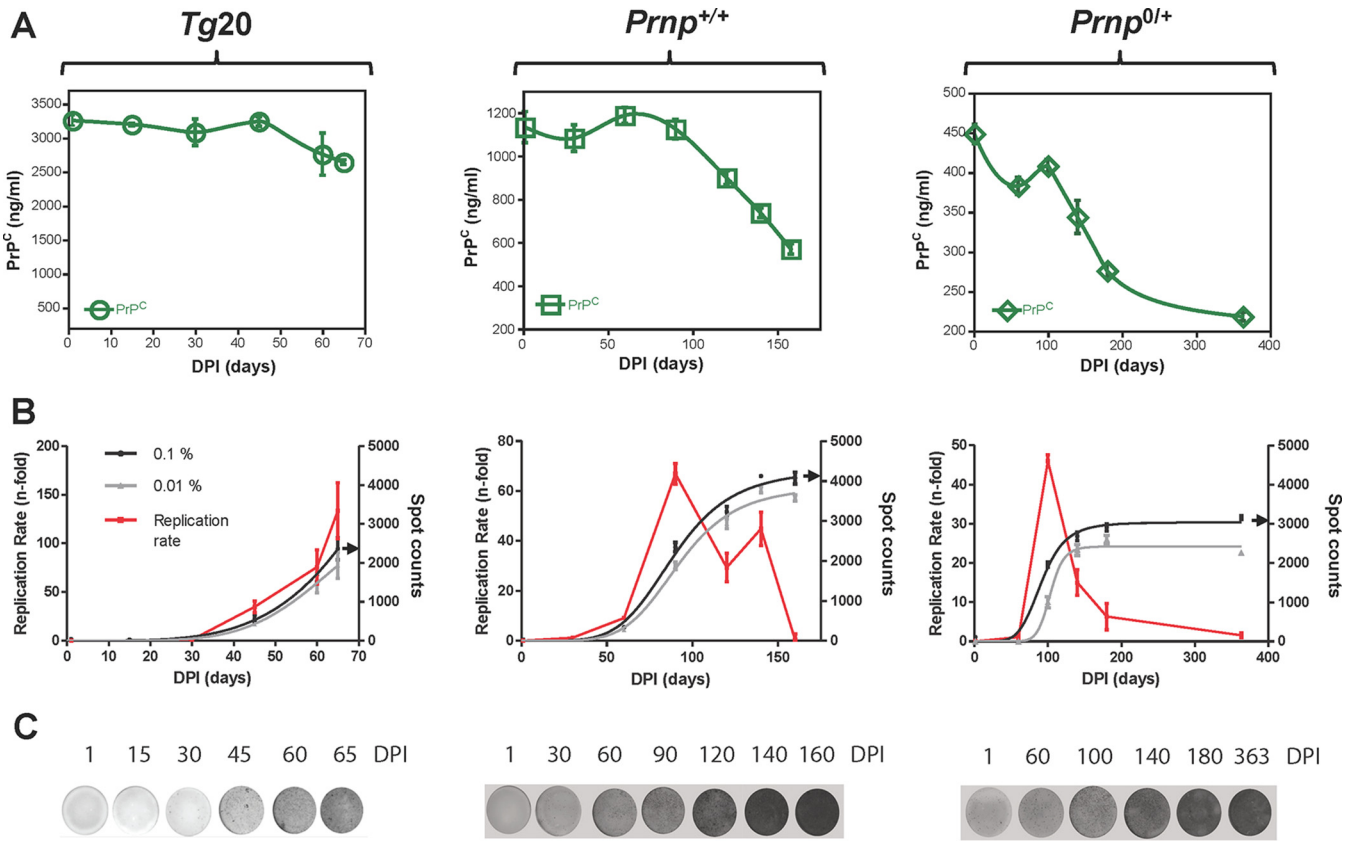

FIG 1 Presence or absence of plateau effects for prion infectivity in three mouse genotypes. (A) PrP^C levels during the time course of RML infection in *Tg20* (Tg.*Prnp*) mice overexpressing the *a* allele of PrP^C, wild-type mice ($Prnp^{+/+}$), and mice hemizygous for the PrP gene ($Prnp^{0/+}$). Note the different scales for the *y* axes. dpi, days postinoculation. Some data points originate from Mays et al. (5). (B) Prion titer in the same time course studies expressed as spot counts per 20,000 cells. SSCA was performed in L929 cells to determine infectivity for brain material in these longitudinal studies of infection (0.1% [wt/vol] homogenate plotted in black; 0.01% homogenate plotted in gray). A red trace depicts the first derivative to represent replication rate for prion titer (spot counts) for the 0.1% (wt/vol) homogenate, with a diminished replication rate being correlated with diminished PrP^C. The data represent averages ± the SEM. Black arrows on the *y* axis indicate maximum of infectivity values by SSCA using 0.1% (wt/vol) homogenate ($n = 8$ to 16). (C) Representative low-power images of the ELISpot wells are presented for each host genotype.

although the replication rates at the last two time points [(75 ± 18)-fold and (133 ± 29)-fold, expressed as means ± the standard errors of the mean (SEM), at 60 and 65 days postinoculation (dpi), respectively] were not significantly different ($P = 0.1$). An infectivity plateau was apparent in the time course for RML infection in *Tg20* mice with sampling every single day between 60 and 65 dpi (2, 3), compared to our sampling on days 60 and 65 dpi. Clear attenuations for the rate of prion replication in wt and hemizy-

TABLE 1 Plateau effects and biophysical parameters of PrP isoforms in prion-infected mice[a]

Parameter	Genotype		
	Tg20 mice (Tg.*Prnp*)	wt mice ($Prnp^{+/+}$)	Hemizygote mice ($Prnp^{0/+}$)
Plateau effect for infectious particles	Equivocal[b]	Equivocal	Yes
Initial PrP^C level (ng/ml)[c]	3,104 ± 190	1,133 ± 15	449 ± 12
Endpoint PrP^C level (ng/ml)	2,760 ± 311	737 ± 5	218 ± 5
Mean percentage of PrP^C ± the SD at the disease end stage (downregulation at disease endpoint)	89% ± 12%	65% ± 3.9%	48% ± 3.3%
Mean infectivity ± the SD at last time point brain material (spots per 20,000 L929 cells)	1,347 ± 157[d]	4,285 ± 254	3,581 ± 270[e]
Specific infectivity of unfractionated brain material (spots per ng of PrP^{Sc})	7.7×10^5	7.7×10^5	7.2×10^5
Gradient fractions with the highest specific infectivity	Low M_r fractions 5 to 9	Low M_r fractions 5 to 9	Low M_r fractions 5 to 9

[a] RML prion strain.
[b] Plateau was described by Sandberg et al. (2, 3); mice were sacrificed every day from 60 dpi onward.
[c] Data obtained from Mays et al. (5).
[d] $P < 0.0001$ (versus $Prnp^{+/+}$ mice).
[e] $P < 0.08$ (versus NS versus $Prnp^{+/+}$ mice).

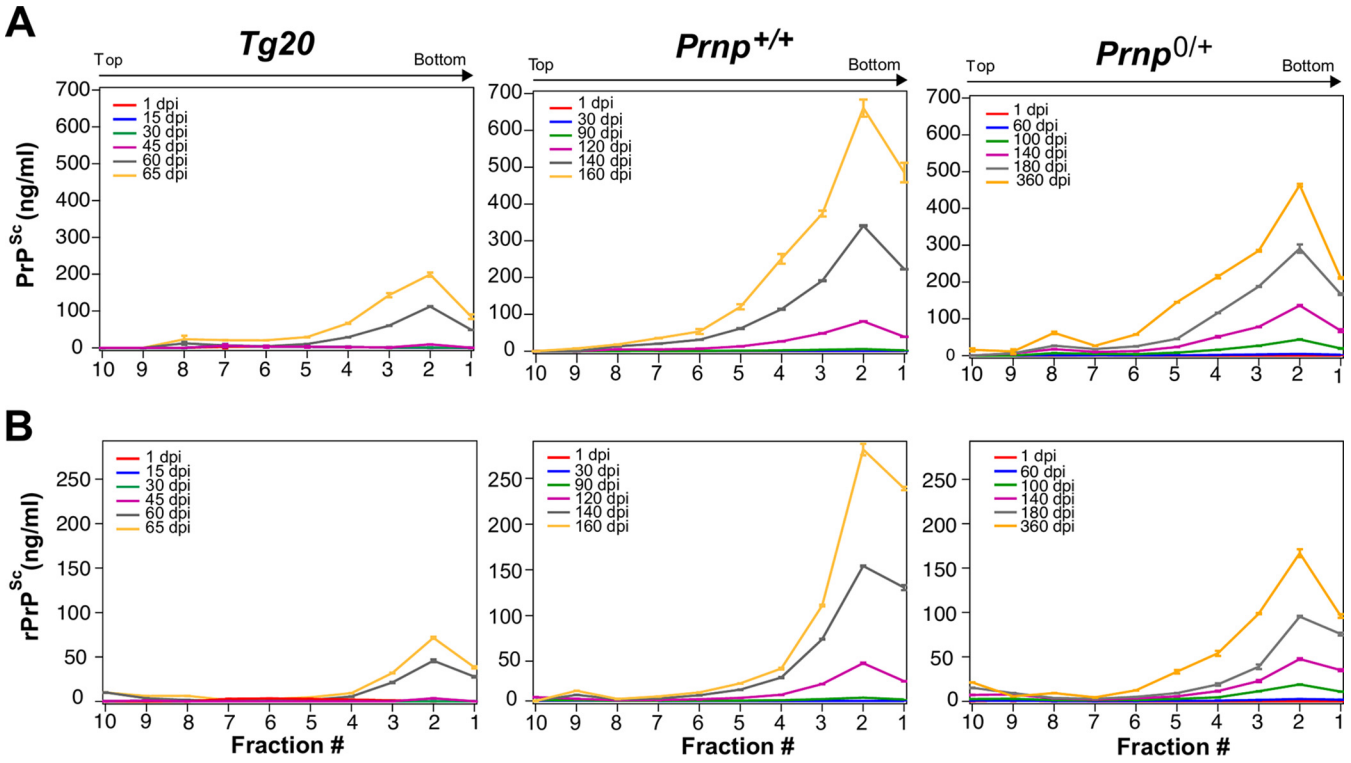

FIG 2 Time course for the appearance of misfolded PrP isoforms in three mouse genotypes. CDI analyses of gradient fractions from brains of mice of three genotypes (*Tg20*, *Prnp*$^{+/+}$, and *Prnp*$^{0/+}$) plotted versus different times after inoculation with the RML prion isolate to represent the gradient profiles for total PrP^{Sc} (A) and rPrP^{Sc} (B) after PK treatment. Time points (dpi) of the source material are indicated within each panel by color codes. Each data point is an average ± the SEM. of triplicate independent CDI measurements in three to four mice brains. CDI values for 30 and 45 dpi for *Tg*20 mice were below assay threshold and are not presented.

gous mice (with an unambiguous plateau in hemizygous mice) were preceded by the occurrence of PrP^{C} downregulation (Fig. 1A and B and Table 1). Although a linear increase in infectivity was recognized between 60 and 140 dpi for wt and hemizygous mice alike (Fig. 1B), continual reductions in PrP^{C} levels apparently prevent substantial increases in infectivity from 140 dpi until terminal disease is reached. For RML-infected wt mice, replication rate fell 58% between 90 and 120 dpi by (69 ± 4)-fold to (29 ± 6)-fold ($P = 0.0001$), whereas the PrP^{C} levels in the same interval dropped by ~20% from 1,124 ± 2 ng/ml to 899 ± 9 ng/ml ($P < 0.01$). For RML-infected hemizygous mice, the changes were greater, such that the replication rate fell 67% between 100 and 140 dpi by (46 ± 1.5)-fold to (15 ± 3.2)-fold ($P = 0.0001$), while the PrP^{C} levels dropped by ~30% from 408 ± 8 ng/ml to 344 ± 21 ng/ml ($P < 0.001$).

Progression of oligomer formation during prion infection. We wanted to determine whether a specific form of PrP, perhaps compatible with the hypothetical species called "PrP^{L}," is responsible for triggering PrP^{C} downregulation and/or a surge of neurotoxicity causing the transition from subclinical disease to neurological end-stage disease. For biophysical analysis, we used velocity gradient centrifugation coupled with CDI to track different PrP species in mice of the aforementioned genotypes at different stages of disease (Fig. 2 and 3). In terms of isoform concentration, higher-molecular-weight species in fraction 2 predominated and increased in a steady manner through the disease course irrespective of the *Prnp* genotype; furthermore, the overall shape of the gradient profiles of PrP^{Sc} and rPrP^{Sc} species did not differ notably as the dpi values increased (Fig. 2). The only possible exception was the emergence of lower-molecular-weight (M_r) species centered on fraction 8 at later time points (most obvious for PrP^{Sc} in hemizygous mice at 363 dpi; Fig. 2, yellow trace, top right-hand panel). To assess this area of the gradient more closely, PrP^{Sc} and rPrP^{Sc} values for fraction 8 (containing oligomeric species) were plotted versus dpi (Fig. 3A). These expanded analyses did not reveal a singular performance for hemizygous mice; rather, they illustrated a spectrum of responses wherein similar levels (~20 ng/ml) of oligomeric PrP^{Sc} accrued at later time points in all three genotypes, but albeit at tempos that varied between the *Tg*20, wt, and hemizygous animals (Fig. 3A). In these analyses, smaller oligomeric forms of PrP assemblies in fraction 8 were more PK-sensitive than large aggregates in fraction 2 (Fig. 3A versus 3B). Lastly, potentially relevant to the triggering of downregulation for wt and hemizygous mice, rPrP^{Sc} species were evident in fraction 2 at time points when PrP^{C} downregulation was already present (at 120 and 140 dpi), respectively (compare Fig. 2A and 3A with Fig. 1A).

Gradient profiles of infectivity during prion infection. As a prelude to extending these types of biophysical analyses to include infectivity measures, measurements of unfractionated brain samples normalized by volume determined that prion infectivity was significantly lower in unfractionated homogenates of *Tg20* mice versus the other two genotypes (Table 1; $P = 0.0001$); this finding is in accord with replication still being in an exponential phase and

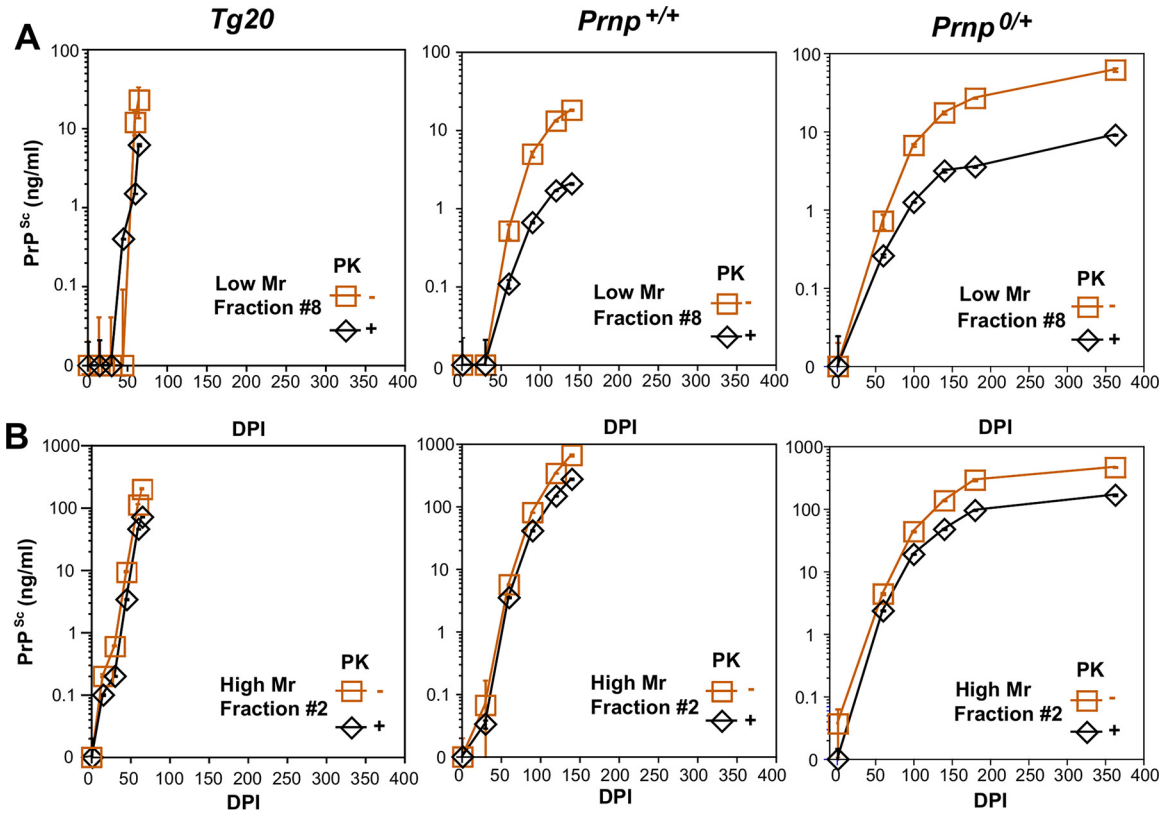

FIG 3 Progressive accumulation of misfolded PrP isoforms in gradient fractions 8 and 2 for three mouse *Prnp* genotypes. (A) Sequential appearance of total PrP^{Sc} and $rPrP^{Sc}$ in fraction 8 containing low-M_r species plotted versus dpi. (B) Sequential appearance of total PrP^{Sc} and $rPrP^{Sc}$ in fraction 2 containing high-M_r species plotted versus dpi. Note the different *y* axes for panels A and B. Each data point is an average ± the SEM of triplicate independent CDI measurements in three to four mice brains. As in Fig. 2, the CDI values for PrP^{Sc} in *Tg20* mice at 30 and 45 days lay below the assay threshold.

thus failing to attain maximum possible values. However, specific infectivity expressed in spots per 20,000 cells per ng of PrP^{Sc} was similar in all three genotypes, indicating that PrP^{C} expression level in the different models did not influence the overall characteristics of the RML prion isolate. Next, we assessed profiles of gradient-fractionated brain lysates for their infectious content in the context of disease time course. Since unfractionated 30 and 45 dpi samples from *Tg20* mice were at the assay baseline, their gradient-fractionated counterparts were not assayed, but we addressed fractionated samples from the last two time points (60 and 65 dpi). For wt mice, we tested the last three time points (120, 140, and 162.67 ± 7.84 dpi) and for hemizygous mice we tested the last four time points (100, 140, 180, and 363 dpi) (Fig. 4A). The data in each fraction was plotted as a specific infectivity value to produce corrected gradient profiles (Fig. 4B). In these corrected analyses, the gradient fractions from terminal *Tg20*, wt, and hemizygous mice closely resembled one another. In each case, the peak of infectivity occurred in either fraction 7 or 8, thus indicating higher infectivity for relatively more PK sensitive, oligomeric PrP^{Sc} in comparison to PK-resistant PrP^{Sc} (Fig. 4B and Table 1). Moreover, within each given genotype, the gradient profile at the last time point did not differ notably in shape from prior time points in the subclinical phase of disease, and the differences in magnitude were an inevitable consequence of alterations in titer over the disease course. A tendency for lower net titers at endpoint in $Prnp^{0/+}$ mice (Fig. 4B) reached significance in 3 of 10 fractions ($P = 0.049$, 0.001, and 0.049, respectively, for fractions 10, 9, and 4). Taken together with the gradient profiles of the PrP isoforms (Fig. 2), our data did not provide evidence of an emergent peak in the infectivity profile or PrP isoform profile that might provide a physiochemical signature for the hypothetical PrP^{L} species. Instead, the data for each genotype revealed gradual alterations in the sedimentation profile favoring the accumulation of small oligomeric forms of PrP (Fig. 4B).

Ratiometric relationship between PrP^{C} downregulation and disease phase. To explore the possible role of oligomers further, we undertook regression analyses. These indicated a statistically significant correlation between incubation time and PrP^{Sc} levels in the low-M_r fraction 8 containing oligomeric species ($R = 0.834$) but not in the high-M_r fraction 2 (Fig. 5). For these analyses, we also included data from a low-copy number Tg.$Prnp^{a}$-AL mouse line (5, 22) infected with the same RML prion isolate. Since PrP^{C} is likely a crucial factor in disease by mediating toxic signaling concentration (23), we next plotted the ratios of residual PrP^{C} to total PrP^{Sc} at the disease endpoint versus the corresponding incubation times using PrP^{Sc} values from either fraction 2 (high M_r) or fraction 8 (low M_r, oligomeric; Fig. 6). Considering these four genotypes infected with the RML prion isolate, the dynamic range of PrP^{C} to PrP^{Sc} ratios extended only from 0.6 to 1.0 for high M_r fractions. However, the dynamic range of ratios expanded ~16-fold (extending from 4.5 to 122) when measuring PrP^{Sc} from oligomeric fractions. Furthermore, this relationship reliably pre-

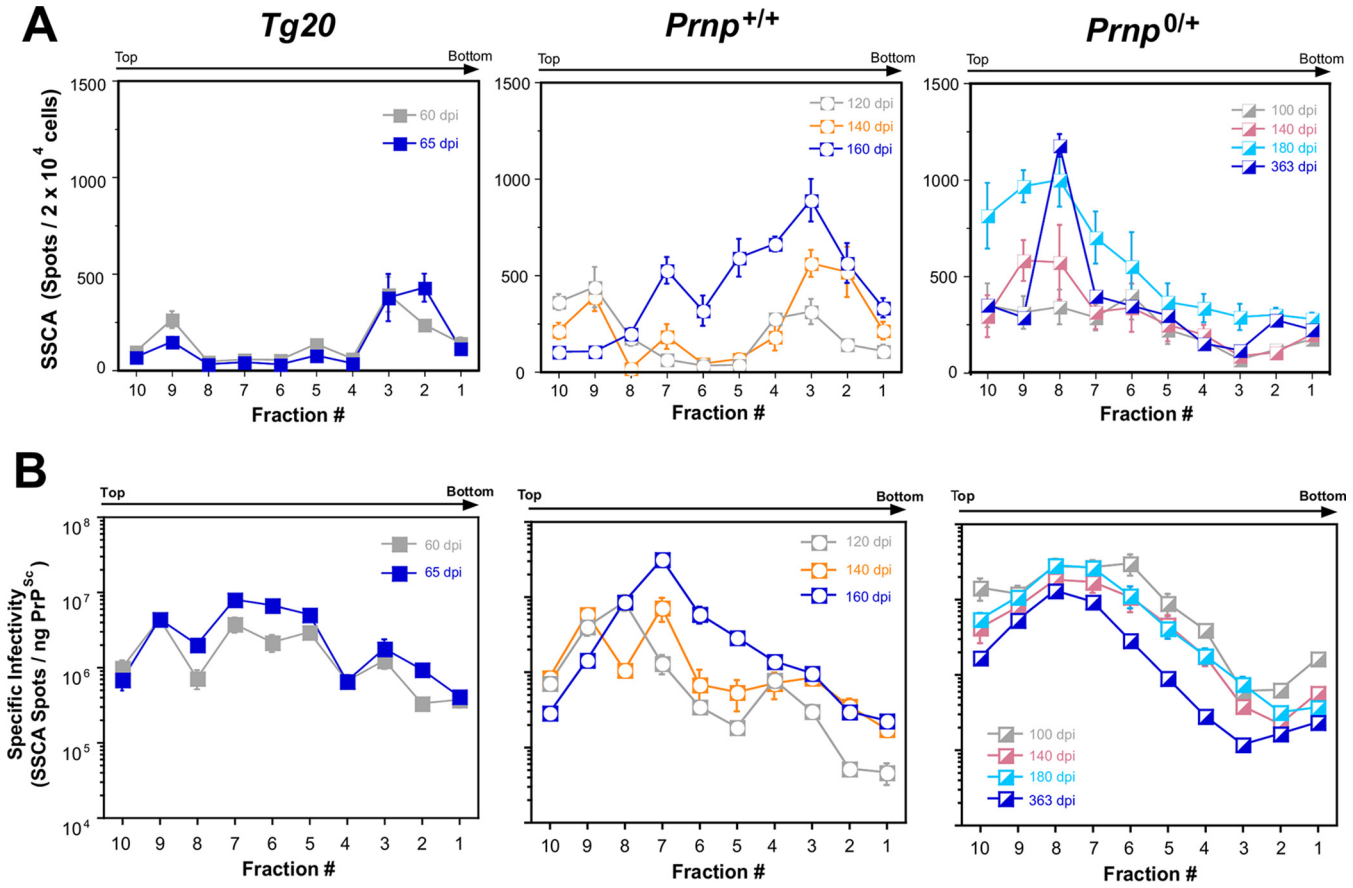

FIG 4 Sequential appearance of infectivity in gradient fractionated material from three *Prnp* genotypes. (A) Uncorrected values for infectivity (spot counts) expressed per unit volume. Note the linear scale for the *y* axis. The infectivity data are averages ± the SEM obtained with 8× to 1× SSCA titrations for each fraction and time point. (B) Specific infectivity of gradient fractions from brains from different time points in disease and with genotypes as indicated.

dicted the incubation time and symptomatic stage of disease with a regression correlation value of 0.998 ($P = 0.004$).

DISCUSSION

In prior theoretical studies, it has been posited that the exponential rate of prion replication eventually inhibits and overtakes prion degradation, although reduced substrate availability simultaneously causes prion replication to decline and prion accumulation to plateau (24). Our study method of velocity gradient fractionation in the presence of Sarkosyl, followed by SSCA and CDI, offers a means to sample diverse PrP species during infection. The data obtained by these methods are summarized in Table 1. Strong effect sizes for PrP^C downregulation in infected wt and hemizygous mice, as well as the synchronicity in reductions in replication rate (Fig. 1), lead us to infer that a relationship exists between PrP^C downregulation and infectivity dropping toward a plateau level during the subclinical phase of prion disease (2, 3). As discussed below, we would assert that this is a simple cause-and-effect relationship. Given that plateau effects can exist, does a hypothetical PrP^L species necessarily follow as a unifying determinant of toxicity and entry into the clinical disease phase? In the experiments here, the PrP allelic type (denoted *Prnp*^{a}) and the prion strain (RML) were held constant and our analyses defined similar profiles after gradient fractionation (Fig. 2A), paralleling the unchanging overall specific infectivity of the samples prior to fractionation (Fig. 4B). The peak for specific infectivity in each case agrees with analyses that the "most infectious" particles (here in fractions 7 and 8) correspond to oligomers rather than high-molecular-weight fibrillar assemblies. These data are in agreement with other velocity gradient analyses (10, 25) and compatible with an analysis where PrP aggregates were dissociated and then fractionated by a native method (26). Importantly, in preclinical samples, the gradient profiles of PrP^{Sc} isoforms detected in a highly sensitive assay and the specific infectivity (Fig. 2 and 4 and Table 1) differed from endpoint samples only in quantity and not quality. A toxic monomeric alpha-helical form of PrP ("TPrP") has been deduced from refolding unglycosylated recombinant PrP and assay upon the PK-1 subline of N2a neuroblastoma cells (27). Toxicity mediated by TPrP was observed in the range of 0.5 to 5 μg/ml (27, 28), which is in the same general range as PrP^C levels measured here in brain homogenates of *Prnp*$^{+/+}$ and *Prnp*$^{0/+}$ mice (i.e., ~1.1 and 0.4 μg/ml, respectively; Fig. 1). Although immunological reagents to distinguish "TPrP" in brain homogenates from PrP^C would facilitate study of this putative toxic alpha-helical form, we already know that the PrP^C levels detected with the 12B2 antibody in *Prnp*$^{+/+}$ and *Prnp*$^{0/+}$ mice are falling—not rising—as animals progress through preclinical disease (to levels of 0.7 and 0.2 μg/ml, respectively, Fig. 1) (5), making a simultaneous, superimposed rise in TPrP levels unlikely. Instead, our data are notable for failing to define a specific form of PrP emerging at

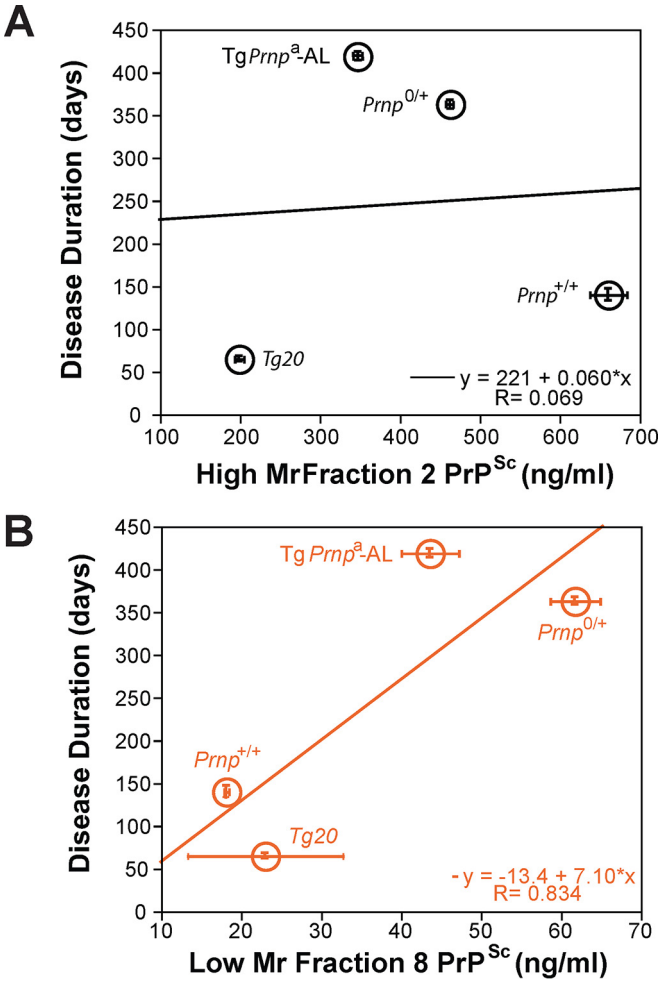

FIG 5 Regression analysis of PrP^{Sc} species in gradient fractions 2 and 8 versus disease incubation time. (A) Regression analysis of high-M_r PrP^{Sc} from gradient fraction 2. (B) Regression analysis of low-M_r oligomeric PrP^{Sc} species from gradient fraction 8.

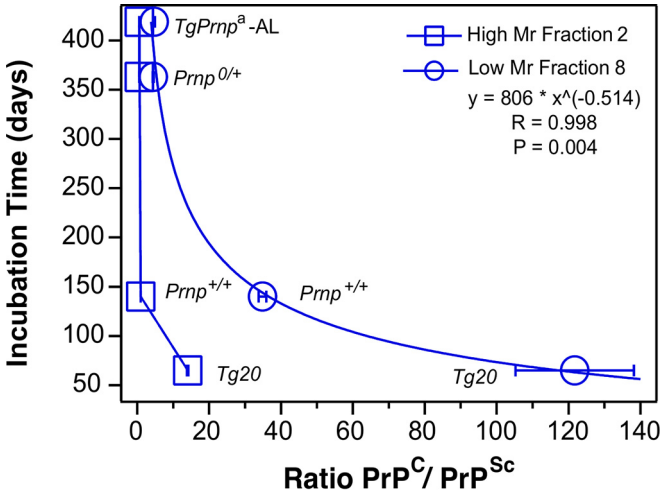

FIG 6 Ratiometric relationship between residual PrP^{C}, $oPrP^{Sc}$, and duration of prion disease. Regression analysis of disease course versus a ratio of residual PrP^{C} concentration at endpoint expressed as a ratio versus concentration of low-M_r (oligomeric) or high-M_r PrP^{Sc}. The infectivity data are averages ± the SEM obtained with 8× to 1× SSCA titrations for each fraction and time point.

the last time points in infection, when the animals exhibit clinical disease. Although our studies did not assay directly for neurotoxicity in cell cultures, the responses in these types of experiments will be dependent upon the particular cells selected. Indeed, it is possible that a protracted search for a hypothetical PrP^{L} molecule might ultimately prove fruitless and that ratios of tangible PrP species are, instead, the critical determinants for disease manifestation. From prior analyses of eight experimental prion diseases at endpoint, we suggested (5) that the entry into and duration of the clinical phase of disease depends on the ratio of PrP^{Sc} to residual PrP^{C} at endpoint. In addition to its role as a substrate, PrP^{C}'s importance here fits with the prior hypothesis that PrP^{C} serves as a PrP^{Sc} receptor to mediate toxic signaling (23, 24). By extending our analyses to include fractionation by velocity gradients, we have identified the low-M_r oligomeric forms of PrP^{Sc} ($oPrP^{Sc}$), rather than high-M_r species, as being particularly important in this ratiometric relationship at the end stage (Fig. 4 to 6). Based on our previous calibrations (10), we estimate the prions in these fractions are assembled from 20 to 78 monomers of PrP^{Sc}.

Returning to consider preclinical events leads to the "whys and wherefores" of downregulation, a process that sculpts PrP^{C}/$oPrP^{Sc}$ ratios. Although cell-based mechanisms to attenuate the accumulation of $rPrP^{Sc}$ or infectivity may exist (for example, clearance [29] and phagocytosis [30]), it is unlikely they could have the same magnitude of impact as the downregulation of PrP^{C}, which is closely linked in time to the drop in replication rate for infectivity and PrP^{Sc} isoforms. This is because (i) PrP^{C} is an obligatory precursor for the formation of PrP^{Sc} and infectivity (shown by the use of PrP transgenic mice [31] and *Prnp*$^{0/0}$ knockout mice [32]) and, conversely, (ii) there is no alternative pathway of cross-seeding to create mouse-adapted prions by misfolding of Sho protein (33–35). Although it remains possible that a particular subpool of PrP^{C} is eligible for conversion to PrP^{Sc} (for example, partially unfolded or particularly glycosylated molecules), the size of this hypothetical pool would have to expand and contract in direct proportion with the net starting concentration of PrP^{C} because constitutive and inducible transgenes that alter PrP^{C} levels have a profound effect upon the generation of prion infectivity and disease incubation times (31, 36, 37). Indeed, altered expression levels of PrP^{C} eclipse the effect of allelic variation that was once thought to be the preeminent determinant of scrapie incubation time in mice (38–40). On a practical level, bulk PrP exists in di-, mono-, and unglycosylated forms, but PrP alleles with amino acid substitutions affecting the attachment of N-glycans are not the equivalent of wt PrP in conversion to PrP^{Sc} after adjusting for expression levels (41–43). During the preclinical downregulation effects that impact PrP^{C} and Sho, the mature glycosylated forms of these proteins are preferentially depleted (5, 44). Furthermore, for Sho, the proportionality of downregulation of mature glycoprotein at endpoint is unaffected by transgene expression levels (44, 45), calling to mind the proportional scaling effect for PrP^{C} expression mentioned above. Overall, we deduce that the supply of mature diglysosylated PrP^{C}, reduced by downregulation versus partial sparing of unglycosylated and monoglycosylated isoforms (5), is a bottleneck for prion replication. Since PrP^{C} is a precursor, this controlling variable inevitably lies "upstream" of all subsequent events. Extending analyses to deal with infectivity (Fig. 1

and Table 1), this concept builds on previous studies that used calibrated *in vitro* reactions to determine the impact of decreasing PrP^C concentration upon decreasing replication rate to make rPrP^{Sc} (5). While we infer that the downregulation of PrP^C and Sho (both glycosylphosphatidylinositol-anchored proteins) triggered by the accumulation of protease resistant PrP (44, 45) might represent a partially effective host response to infection, interventions to further depress PrP^C may have the benefit of reducing plateau values for infectivity, extending the length of subclinical disease and the amount of residual cell surface molecules available to transduce the toxic effects of misfolded PrPs.

Cumulatively, our measurements in three mouse genotypes infected with the RML prion strain failed to define a consistent plateau phenomenon, but rather data that existed on a continuum with dropping levels of PrP^C being crucial in the asymptomatic phase of disease. Rising levels of mobile small oligomeric prions can then transform this phase of prion disease into a symptomatic stage at the threshold ratio between available PrP^C and oPrP^{Sc} (Fig. 6). These aspects argue for dynamic interactions, where fewer small oligomeric prions are able to trigger symptoms at high surface cell concentrations of PrP^C, receptors for toxicity, and vice versa.

ACKNOWLEDGMENTS

We thank Witold Surewicz for recombinant PrP used for calibration in CDI, Earl Poptic from Cleveland Clinic Hybridoma Core Facility for the production of 8H4 MAb, and J. Langeveld for providing 12B2 MAb (epitope 88-92). We thank F. Jirik (University of Calgary, Calgary, Alberta, Canada) and V. Sim (University of Alberta) for *Tg20* mice and J. Yang, J. Grams, and K. Bergen for maintenance of the mouse colony.

This study was supported by grants from the National Institute for Neurological Disorders and Stroke (NS074317), the Centers for Disease Control and Prevention (UR8/CCU515004), the Charles S. Britton Fund, the Canada Foundation for Innovation, the Canadian Institutes of Health Research (MOP36377), the Alberta Prion Research Institute, and Alberta Innovates-Health Solutions (through a postdoctoral fellowship supporting C.E.M.).

Experiments were designed by C.E.M., J.V.D.M., and D.W. Experiments were performed and analyzed by C.E.M., J.V.D.M., C.K., T.H., D.M., J.G.S., and D.W. The manuscript was written by C.E.M., J.G.S., and D.W.

REFERENCES

1. **Prusiner SB.** 1998. Prions. Proc Natl Acad Sci U S A **95:**13363–13383. http://dx.doi.org/10.1073/pnas.95.23.13363.
2. **Sandberg MK, Al-Doujaily H, Sharps B, Clarke AR, Collinge J.** 2011. Prion propagation and toxicity in vivo occur in two distinct mechanistic phases. Nature **470:**540–542. http://dx.doi.org/10.1038/nature09768.
3. **Sandberg MK, Al-Doujaily H, Sharps B, De Oliveira MW, Schmidt C, Richard-Londt A, Lyall S, Linehan JM, Brandner S, Wadsworth JDF, Clarke AR, Collinge J.** 2014. Prion neuropathology follows the accumulation of alternate prion protein isoforms after infective titre has peaked. Nat Commun **5:**4347. http://dx.doi.org/10.1038/ncomms5347.
4. **Büeler H, Raeber A, Sailer A, Fischer M, Aguzzi A, Weissmann C.** 1994. High prion and PrPSc levels but delayed onset of disease in scrapie-inoculated mice heterozygous for a disrupted PrP gene. Mol Med **1:**19–30.
5. **Mays CE, Kim C, Haldiman T, van der Merwe J, Lau A, Yang J, Grams J, Di Bari MA, Nonno R, Telling GC, Kong Q, Langeveld J, McKenzie D, Westaway D, Safar JG.** 2014. Prion disease tempo determined by host-dependent substrate reduction. J Clin Invest **124:**847–858. http://dx.doi.org/10.1172/JCI72241.
6. **Saborio GP, Permanne B, Soto C.** 2001. Sensitive detection of pathological prion protein by cyclic amplification of protein misfolding. Nature **411:**810–813. http://dx.doi.org/10.1038/35081095.
7. **Castilla J, Morales R, Saá P, Barria M, Gambetti P, Soto C.** 2008. Cell-free propagation of prion strains. EMBO J **27:**2557–2566. http://dx.doi.org/10.1038/emboj.2008.181.
8. **Fischer M, Rulicke T, Raeber A, Sailer A, Moser M, Oesch B, Brandner S, Aguzzi A, Weissmann C.** 1996. Prion protein (PrP) with amino-proximal deletions restoring susceptibility of PrP knockout mice to scrapie. EMBO J **15:**1255–1264.
9. **Safar J, Wille H, Itri V, Groth D, Serban H, Torchia M, Cohen FE, Prusiner SB.** 1998. Eight prion strains have PrP^{Sc} molecules with different conformations. Nat Med **4:**1157–1165. http://dx.doi.org/10.1038/2654.
10. **Kim C, Haldiman T, Surewicz K, Cohen Y, Chen W, Blevins J, Sy M-S, Cohen M, Kong Q, Telling GC, Surewicz WK, Safar JG.** 2012. Small protease sensitive oligomers of PrPSc in distinct human prions determine conversion rate of PrPC. PLoS Pathog **8:**e1002835. http://dx.doi.org/10.1371/journal.ppat.1002835.
11. **Safar JG, Geschwind MD, Deering C, Didorenko S, Sattavat M, Sanchez H, Serban A, Vey M, Baron H, Giles K, Miller BL, DeArmond SJ, Prusiner SB.** 2005. Diagnosis of human prion disease. Proc Natl Acad Sci U S A **102:**3501–3506. http://dx.doi.org/10.1073/pnas.0409651102.
12. **Kim C, Haldiman T, Cohen Y, Chen W, Blevins J, Sy M-S, Cohen M, Safar JG.** 2011. Protease-sensitive conformers in broad spectrum of distinct PrPSc structures in sporadic Creutzfeldt-Jakob disease are indicator of progression rate. PLoS Pathog **7:**e1002242. http://dx.doi.org/10.1371/journal.ppat.1002242.
13. **Safar JG, Lessard P, Tamgüney G, Freyman Y, Deering C, Letessier F, DeArmond SJ, Prusiner SB.** 2008. Transmission and detection of prions in feces. J Infect Dis **198:**81–89. http://dx.doi.org/10.1086/588193.
14. **Safar JG, Scott M, Monaghan J, Deering C, Didorenko S, Vergara J, Ball H, Legname G, Leclerc E, Solforosi L, Serban H, Groth D, Burton DR, Prusiner SB, Williamson RA.** 2002. Measuring prions causing bovine spongiform encephalopathy or chronic wasting disease by immunoassays and transgenic mice. Nat Biotechnol **20:**1147–1150. http://dx.doi.org/10.1038/nbt748.
15. **Thackray AM, Hopkins L, Bujdoso R.** 2007. Proteinase K-sensitive disease-associated ovine prion protein revealed by conformation-dependent immunoassay. Biochem J **401:**475–483. http://dx.doi.org/10.1042/BJ20061264.
16. **Bellon A, Seyfert-Brandt W, Lang W, Baron H, Gröner A, Vey M.** 2003. Improved conformation-dependent immunoassay: suitability for human prion detection with enhanced sensitivity. J Gen Virol **84:**1921–1925. http://dx.doi.org/10.1099/vir.0.18996-0.
17. **Choi YP, Gröner A, Ironside JW, Head MW.** 2011. Comparison of the level, distribution and form of disease-associated prion protein in variant and sporadic Creutzfeldt-Jakob diseased brain using conformation-dependent immunoassay and Western blot. J Gen Virol **92:**727–732. http://dx.doi.org/10.1099/vir.0.026948-0.
18. **McCutcheon S, Hunter N, Houston F.** 2005. Use of a new immunoassay to measure PrPSc levels in scrapie-infected sheep brains reveals PrP genotype-specific differences. J Immunol Methods **298:**119–128. http://dx.doi.org/10.1016/j.jim.2005.01.012.
19. **Zanusso G, Liu D, Ferrari S, Hegyi I, Yin X, Aguzzi A, Hornemann S, Liemann S, Glockshuber R, Manson JC, Brown P, Petersen RB, Gambetti P, Sy MS.** 1998. Prion protein expression in different species: analysis with a panel of new MAbs. Proc Natl Acad Sci U S A **95:**8812–8816. http://dx.doi.org/10.1073/pnas.95.15.8812.
20. **Langeveld JPM, Jacobs JG, Erkens JHF, Bossers A, Zijderveld FG, van Keulen LJM.** 2006. Rapid and discriminatory diagnosis of scrapie and BSE in retro-pharyngeal lymph nodes of sheep. BMC Vet Res **9:**19.
21. **van der Merwe J, Aiken J, Westaway D, McKenzie D.** 2015. The standard scrapie cell assay: development, utility and prospects. Viruses **7:**180–198. http://dx.doi.org/10.3390/v7010180.
22. **Lau A, McDonald A, Daude N, Mays CE, Walter ED, Aglietti R, Mercer RCC, Wohlgemuth S, van der Merwe J, Yang J, Gapeshina H, Kim C, Grams J, Shi B, Wille H, Balachandran A, Schmitt-Ulms G, Safar JG, Millhauser GL, Westaway D.** 2015. Octarepeat region flexibility impacts prion function, endoproteolysis, and disease manifestation. EMBO Mol Med **7:**339–356. http://dx.doi.org/10.15252/emmm.201404588.
23. **Brandner S, Isenmann S, Raeber A, Fischer M, Sailer A, Kobayashi Y, Marino S, Weismann C, Aguzzi A.** 1996. Normal host prion protein necessary for scrapie-induced neurotoxicity. Nature **379:**339–343. http://dx.doi.org/10.1038/379339a0.
24. **Aguzzi A, Falsig J.** 2012. Prion propagation, toxicity and degradation. Nat Neurosci **15:**936–939. http://dx.doi.org/10.1038/nn.3120.
25. **Tixador P, Herzog L, Reine F, Jaumain E, Chapuis J, Le Dur A, Laude**

H, Béringue V. 2010. The physical relationship between infectivity and prion protein aggregates is strain dependent. PLoS Pathog **6:**e1000859. http://dx.doi.org/10.1371/journal.ppat.1000859.
26. **Silveira JR, Raymond GJ, Hughson AG, Race RE, Sim VL, Hayes SF, Caughey B.** 2005. The most infectious prion protein particles. Nature **437:**257–261. http://dx.doi.org/10.1038/nature03989.
27. **Zhou M, Ottenberg G, Sferrazza GF, Lasmézas CI.** 2012. Highly neurotoxic monomeric α-helical prion protein. Proc Natl Acad Sci U S A **109:**3113–3118. http://dx.doi.org/10.1073/pnas.1118090109.
28. **Zhou M, Ottenberg G, Sferrazza GF, Hubbs C, Fallahi M, Rumbaugh G, Brantley AF, Lasmézas CI.** 2015. Neuronal death induced by misfolded prion protein is due to NAD^+ depletion and can be relieved in vitro and in vivo by NAD^+ replenishment. Brain **138:**992–1008. http://dx.doi.org/10.1093/brain/awv002.
29. **Safar JG, DeArmond SJ, Kociuba K, Deering C, Didorenko S, Bouzamondo-Bernstein E, Prusiner SB, Tremblay P.** 2005. Prion clearance in bigenic mice. J Gen Virol **86:**2913–2923. http://dx.doi.org/10.1099/vir.0.80947-0.
30. **Brown GC, Neher JJ.** 2014. Microglial phagocytosis of live neurons. Nat Rev Neurosci **15:**209–216. http://dx.doi.org/10.1038/nrn3710.
31. **Prusiner SB, Scott M, Foster D, Pan K-M, Groth D, Mirenda C, Torchia M, Yang S-L, Serban D, Carlson GA, Hoppe PC, Westaway D, DeArmond SJ.** 1990. Transgenetic studies implicate interactions between homologous PrP isoforms in scrapie prion replication. Cell **63:**673–686. http://dx.doi.org/10.1016/0092-8674(90)90134-Z.
32. **Büeler H, Aguzzi A, Sailer A, Greiner R-A, Autenried P, Aguet M, Weissmann C.** 1993. Mice devoid of PrP are resistant to scrapie. Cell **73:**1339–1347. http://dx.doi.org/10.1016/0092-8674(93)90360-3.
33. **Premzl M, Sangiorgio L, Strumbo B, Marshall Graves JA, Simonic T, Gready JE.** 2003. Shadoo, a new protein highly conserved from fish to mammals and with similarity to prion protein. Gene **314:**89–102. http://dx.doi.org/10.1016/S0378-1119(03)00707-8.
34. **Watts JC, Drisaldi B, Ng V, Yang J, Strome B, Horne P, Sy MS, Yoong L, Young R, Mastrangelo P, Bergeron C, Fraser PE, Carlson GA, Mount HT, Schmitt-Ulms G, Westaway D.** 2007. The CNS glycoprotein Shadoo has PrP(C)-like protective properties and displays reduced levels in prion infections. EMBO J **26:**4038–4050. http://dx.doi.org/10.1038/sj.emboj.7601830.
35. **Daude N, Wohlgemuth S, Brown R, Pitstick R, Gapeshina H, Yang J, Carlson GA, Westaway D.** 2012. Knockout of the prion protein (PrP)-like Sprn gene does not produce embryonic lethality in combination with PrPC deficiency. Proc Natl Acad Sci U S A **109:**9035–9040. http://dx.doi.org/10.1073/pnas.1202130109.
36. **Carlson GA, Ebeling C, Yang S-L, Telling G, Torchia M, Groth D, Westaway D, DeArmond SJ, Prusiner SB.** 1994. Prion isolate specified allotypic interactions between the cellular and scrapie prion proteins in congenic and transgenic mice. Proc Natl Acad Sci U S A **91:**5690–5694. http://dx.doi.org/10.1073/pnas.91.12.5690.
37. **Mallucci G, Dickinson A, Linehan J, Klöhn P-C, Brandner S, Collinge J.** 2003. Depleting neuronal PrP in prion infection prevents disease and reverses spongiosis. Science **302:**871–874. http://dx.doi.org/10.1126/science.1090187.
38. **Dickinson AG, Fraser H.** 1979. An assessment of the genetics of scrapie in sheep and mice, p 367–386. *In* Prusiner SB, Hadlow WJ (ed), Slow transmissible diseases of the nervous system, vol 1. Academic Press, Inc, New York, NY.
39. **Westaway D, Mirenda CA, Foster D, Zebarjadian Y, Scott M, Torchia M, Yang S-L, Serban H, DeArmond SJ, Ebeling C, Prusiner SB, Carlson GA.** 1991. Paradoxical shortening of scrapie incubation times by expression of prion protein transgenes derived from long incubation period mice. Neuron **7:**59–68. http://dx.doi.org/10.1016/0896-6273(91)90074-A.
40. **Moore RC, Hope J, McBride PA, McConnell I, Selfridge J, Melton DW, Manson JC.** 1998. Mice with gene targetted prion protein alterations show that *Prnp*, *Sinc*, and *Prni* are congruent. Nat Genet **18:**118–125. http://dx.doi.org/10.1038/ng0298-118.
41. **Rogers M, Taraboulos A, Scott M, Borchelt D, Serban D, Gyuris T, Prusiner SB.** 1992. Modification and expression of prion proteins in cultured cells, p 457–469. *In* Prusiner SB, Collinge J, Powell J, Anderton B (ed), Prion diseases of humans and animals. Ellis Horwood, London, United Kingdom.
42. **Neuendorf E, Weber A, Saalmueller A, Schatzl H, Reifenberg K, Pfaff E, Groschup MH.** 2004. Glycosylation deficiency at either one of the two glycan attachment sites of cellular prion protein preserves susceptibility to bovine spongiform encephalopathy and scrapie infections. J Biol Chem **279:**53306–53316. http://dx.doi.org/10.1074/jbc.M410796200.
43. **Tuzi NL, Cancellotti E, Baybutt H, Blackford L, Bradford B, Plinston C, Coghill A, Hart P, Piccardo P, Barron RM, Manson JC.** 2008. Host PrP glycosylation: a major factor determining the outcome of prion infection. PLoS Biol **6:**e100. http://dx.doi.org/10.1371/journal.pbio.0060100.
44. **Westaway D, Genovesi S, Daude N, Brown R, Lau A, Lee I, Mays CE, Coomaraswamy J, Canine B, Pitstick R, Herbst A, Yang J, Ko KWS, Schmitt-Ulms G, DeArmond SJ, McKenzie D, Hood L, Carlson GA.** 2011. Downregulation of Shadoo in prion infections traces a preclinical event inversely related to PrP^{Sc} accumulation. PLoS Pathog **7:**e1002391. http://dx.doi.org/10.1371/journal.ppat.1002391.
45. **Watts JC, Stöhr J, Bhardwaj S, Wille H, Oehler A, DeArmond SJ, Giles K, Prusiner SB.** 2011. Protease-resistant prions selectively decrease Shadoo protein. PLoS Pathog **7:**e1002382. http://dx.doi.org/10.1371/journal.ppat.1002382.